European Journal of Chemistry 16 (2) (2025) 169-177

European Journal of Chemistry

Synthesis, characterization, and antimicrobial activity of Cu(II) and Zn(II) complexes with *N*,*N*-bis(4-methoxybenzylidene)ethylenediamine or *N*-(4-methoxybenzylidene)ethylenediamine Schiff base

Adrienne Ndiolene [1], Tidiane Diop [1,*], Mouhamadou Sembene Boye [2], Bruno Faure [3], Aminata Diasse-Sarr [1] and Michel Giorgi [4]

[1] *Département de Chimie, Université Cheikh Anta Diop de Dakar, BP 5005 Fan-Dakar, Sénégal*
[2] *Département de Physique Chimie, Faculté des Sciences et Technologies de l'Education et de la Formation, Université Cheikh Anta Diop, Boulevard Habib, Bourguiba, BP 5036 Fann-Dakar, Sénégal*
[3] *ISM2 - Institut des Sciences Moléculaires de Marseille, Campus Saint Jérôme Av. escadrille Normandie Niemen BP 531 13397 Marseille Cedex 20, France*
[4] *AMU SPEC - Spectropôle - Aix Marseille Université, Campus Scientifique de Saint Jérôme Service 511 13397 Marseille Cedex 20, France*

* *Corresponding author at: Département de Chimie, Université Cheikh Anta Diop de Dakar, BP 5005 Fan-Dakar, Sénégal.*
e-mail: tidiane3.diop@ucad.edu.sn (T. Diop).

RESEARCH ARTICLE

10.5155/eurjchem.16.2.169-177.2651

Received: 22 January 2025
Received in revised form: 26 March 2025
Accepted: 2 May 2025
Published online: 30 June 2025
Printed: 30 June 2025

KEYWORDS

Synthesis
Schiff base
Characterization
Crystal structure
Antimicrobial activity
Cu(II) and Zn(II) complexes

ABSTRACT

Seven mononuclear complexes were synthesized by mixing *N*,*N*'-bis(4-methoxy benzaldehyde)ethylenediamine (L) or *N*-(4-methoxybenzylidene)ethylenediamine (L_1) and copper or zinc salts. These compounds were characterized by IR, ^{1}H NMR, UV-vis, fluorescence spectroscopy, molar conductimetric, and elemental (CHN) analysis techniques. The crystal structures of the zinc complexes were determined by single crystal X-ray diffraction studies. Crystal data for $C_{18}H_{20}I_2N_2O_2Zn$: Monoclinic, space group $P2_1/c$ (no. 14), a = 10.45670(10) Å, b = 13.28610(10) Å, c = 15.43490(10) Å, β = 96.4300(10)°, V = 2130.86(3) Å^3, Z = 4, $Dcalc$ = 1.919 g/cm^3, 46801 reflections measured ($8.51° \leq 2\Theta \leq 145.92°$), 4231 unique ($R_{int}$ = 0.0565, R_{sigma} = 0.0185) which were used in all calculations. Crystal data for $C_{18}H_{20}Br_2N_2O_2Zn$: Monoclinic, space group $P2_1/c$ (no. 14), a = 10.30071(17) Å, b = 13.00839(18) Å, c = 15.0084(2) Å, β = 97.3057(14) °, V = 1994.74(5) Å^3, Z = 4, $Dcalc$ = 1.737 g/cm^3, 103282 reflections measured ($4.158° \leq 2\Theta \leq 59.492°$), 5360 unique ($R_{int}$ = 0.0394, R_{sigma} = 0.0161) which were used in all calculations. Crystal structures show a distorted tetrahedral geometry around the zinc metal. The ligand is bidentate chelating with imine nitrogen atoms. Fluorescence spectroscopy shows a reduction in the fluorescence intensity of the complexes relative to the ligand. This reduction is due to the presence of metal-coordinated halides. The *in vitro* antimicrobial activities of the ligand and complexes were elaborated by screening them against Gram(+) bacteria (*Streptococcus pyogenes*), Gram(-) bacteria (*Pseudomonas aeruginosa),* and a fungus (*Candida albicans*). All compounds showed weak activity against the tested bacterial and fungal strains.

Cite this: *Eur. J. Chem.* **2025**, *16(2)*, 169-177 **Journal website**: www.eurjchem.com

1. Introduction

Schiff bases derived from primary amines are excellent chelating agents for metal ions *via* azomethine nitrogen (>C=N-) [1-4]. Metal complexes with Schiff bases have antibacterial, antifungal, antitumor, and antianalgesic activities [5-9]. Macrocyclic derivatives of Schiff bases have countless ultimate functions, such as photosynthesis, oxygen transport in mammals, and other respiratory patterns [10]. A considerable number of Schiff base complexes have been used as biological models to understand the structure of biomolecules and biological processes [11]. These compounds are active against a wide range of organisms such as *Candida albicans*, *Escherichia coli*, *Staphylococcus aureus*, *Bacillus polymxa*, *Trychophyton gypseum*, *Mycobacteria*, *Erysiphe graminis,* and *Plasmopara viticola* [12-16]. In recent years, zinc compounds with a stable d^{10} electronic configuration have received considerable attention in the fields of inorganic chemistry, biochemistry, and environmental chemistry. Approximately ten zinc-based enzymes are known, in which zinc is generally tetrahedral and is linked to donor nitrogen atoms [17,18]. In this work, Cu(II) and Zn(II) complexes with symmetric Schiff bases of ethylenediamine and benzaldehyde (4-methoxybenzaldehyde) were synthesized to explore their antimicrobial activity.

2. Experimental

2.1. Instrumentation

The elemental analyses for carbon, hydrogen, and nitrogen of the metal complexes were carried out using a Flash EA 1112 Elementary Analyzer. Electronic spectra were recorded with a CARY 50 BIO UV-Vis spectrometer from 200 to 800 nm. The ^{1}H and ^{13}C NMR spectra were recorded on a Bruker AV2 (400 MHz) spectrometer using DMSO-d_6 as a solvent.

ISSN 2153-2249 (Print) / ISSN 2153-2257 (Online)
https://dx.doi.org/10.5155/eurjchem.16.2.169-177.2651

Table 1. Crystal data and structure refinement for the zinc complexes.

Compound	**A_6**	**A_7**
Empirical formula	$C_{18}H_{20}I_2N_2O_2Zn$	$C_{18}H_{20}Br_2N_2O_2Zn$
Formula weight (g/mol)	615.53	521.55
Temperature (K)	295	295
Crystal system	Monoclinic	Monoclinic
Space group	$P2_1/c$	$P2_1/c$
a (Å)	10.45670(10)	10.30071(17)
b (Å)	13.28610(10)	13.00839(18)
c (Å)	15.43490(10)	15.0084(2)
α (°)	90	90
β (°)	96.4300(10)	97.3057(14)
γ (°)	90	90
Volume (Å^3)	2130.86(3)	1994.74(5)
Z	4	4
ρ_{calc} (g/cm^3)	1.919	1.737
μ (mm^{-1})	24.455	5.251
F(000)	1176.0	1032.0
Crystal size (mm^3)	0.2 × 0.08 × 0.08	0.26 × 0.26 × 0.08
Radiation	Cu Kα (λ = 1.54184)	Mo Kα (λ = 0.71073)
2Θ range for data collection (°)	8.51 to 145.92	4.158 to 59.492
Index ranges	$-12 \le h \le 12, -16 \le k \le 16, -19 \le l \le 19$	$-13 \le h \le 14, -17 \le k \le 17, -20 \le l \le 20$
Reflections collected	46801	103282
Independent reflections	4231 [R_{int} = 0.0565, R_{sigma} = 0.0185]	5360 [R_{int} = 0.0394, R_{sigma} = 0.0161]
Data/restraints/parameters	4231/0/228	5360/0/228
Goodness-of-fit on F^2	1.045	1.023
Final R indexes [I≥2σ (I)]	R_1 = 0.0359, wR_2 = 0.0980	R_1 = 0.0285, wR_2 = 0.0589
Final R indexes [all data]	R_1 = 0.0374, wR_2 = 0.1000	R_1 = 0.0462, wR_2 = 0.0650
Largest diff. peak/hole (e.Å^{-3})	1.42/-0.65	0.69/-0.55

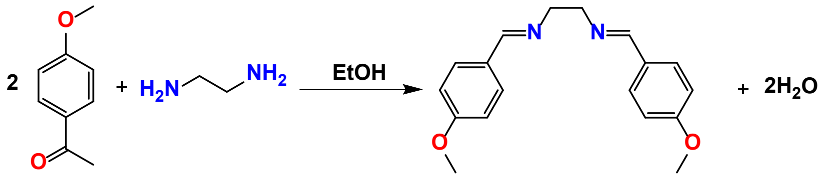

Scheme 1. Synthesis of the ligand *N*,*N'*-bis(4-methoxybenzaldehyde)ethylenediamine.

The IR spectra were recorded in the region 4000-200 cm^{-1} by using a FT-IR Bruker Tensor 27 spectrometer and fluorescence spectra were recorded on a Horiba Jobin Ivon Fluoromax-4 spectrofluorometer. X-ray diffraction measurements of Zn(II) complexes were performed using a SuperNova Dual AtlasS2 diffractometer with graphite-monochromated CuKα radiation (λ = 1.54184 Å) for complex A_6 and MoKα radiation (λ = 0.71073 Å) for complex A_7. The structures were solved by direct methods with SHELXT [19] using Olex2 [20]. structure solution program using intrinsic phasing and refined with the SHELXL [19] refinement package using least squares minimization. The experimental parameters related to single-crystal X-ray analysis of complexes are given in Table 1.

2.2. Synthesis

2.2.1. Synthesis of the Schiff base (L)

The Schiff base ligand (L) was synthesized by mixing solutions of ethylenediamine (30 mmol; 1.8 g) and *para*-anisaldehyde (60 mmol; 8.169 g) in 30 mL of ethanol (Scheme 1). The yellow mixture obtained, stirring, is brought to reflux for 5 hours at a temperature of 80 °C, then filtered and placed under slow evaporation. After a few days, a mass of 6.345 g of crystals is obtained with a yield of 80.9% [21].

2.2.2. General procedure for the synthesis of the complexes

The metal complexes were synthesized by reacting a methanolic solution of ligand L (296.36 mg, 1 mmol) with an equimolar amount of the corresponding metal salt in a 1:1 molar ratio. The reaction mixture was stirred for 3 hours at room temperature. For the zinc chloride complex (A_4), 0.296 g (1 mmol) of L was dissolved in 96% ethanol, followed by the addition of 1 mmol of zinc chloride. The mixture was refluxed at 80 °C for 21 hours. After stirring for two hours, the precipitates were filtered, washed, and dried, while the filtrates were subjected to slow evaporation (Table 2). The melting temperatures of the synthesized complexes were determined as follows: $[Cu(L)(ClO_4)(CH_3OH)]\cdot ClO_4$ (A_1) melted at 184.0 °C, $[Cu(L)(CH_3COO)_2]\cdot 3H_2O$ (A_2) at 189.7 °C, and $[Cu(L_1)Cl_2]\cdot H_2O$ (A_3) at 216.0 °C. The complexes $[Zn(L)Cl_2]$ (A_5), $[Zn(L)I_2]$ (A_6) and $[Zn(L)Br_2]$ (A_7) exhibited melting temperatures of 235.4 °C, 207.2 °C, and 235.9 °C, respectively. The powders of A4, A5, A6, and A7 were recrystallized from methanol, and the resulting crystals were analyzed by X-ray diffraction [22]. *N*-(4-Methoxybenzylidene)ethylenediamine ligand (L) was obtained in situ by hydrolysis of *N*,*N*-bis(4-methoxybenzylidene) ethylenediamine ligand (L_1).

2.3. Antimicrobial activity

The antibacterial activity of the ligand and its metal complexes was determined against two wild-type bacterial strains responsible for certain serious infectious diseases: a Gram-negative strain (*Pseudomonas aeruginosa*) and a Gram-positive strain (*Streptococcus pyogenes*). The fungus used for antifungal activity is *Candida albican*. The solutions of the ligand and their complexes were prepared in DMSO at concentrations 100, 50, 30 and 25 mM. The evaluation of the preliminary antibacterial and antifungal effect of the Schiff base ligand and these metal derivatives is carried out by the method of serial dilution in microplates according to the recommendations of the protocol described in a previous study [23]. Bacteria (*Pseudomonas aeruginosa* and *Streptococcus pyogenes*) and the fungus (*Candida albicans* DSM) were exposed to increasing concentrations of complexes and ligand with a final volume of each well equal to 150 µL.

Table 2. Main characteristics of complexes derived from L *.

Complex	Metal salt	Color and nature	Yield (%)	Found (Calcd.) %		
				C	H	N
$[Cu(L)(ClO_4)(CH_3OH)]\cdot ClO_4$ (A_1)	Copper(II) perchlorate	Blue (Powder)	79.42	38.55(38.62)	4.12(4.09)	3.77(4.74)
$[Cu(L)(CH_3COO)_2]\cdot 3H_2O$ (A_2)	Copper(II)acetate	Blue (Powder)	68.51	48.20(49.66)	5.62(6.06)	6.61(5.27)
$[Cu(L_1)Cl_2]\cdot H_2O$ (A_3)	Copper(II) chloride	Blue (Powder)	36.44	36.53(36.32)	4.59(4.88)	8.97(8.47)
$[Zn(L_1)Cl_2]$ (A_4)	Zinc chloride	Yellow (Crystal)	61.00	-	-	-
$[Zn(L)Cl_2]$ (A_5)	Zinc chloride	Yellow (Crystal)	38.34	49.87(49.97)	4.67(4.66)	6.49(6.47)
$[Zn(L)I_2]$ (A_6)	Zinc iodide	Yellow (Crystal)	56.30	34.90(35.12)	3.26(3.27)	4.48(4.55)
$[Zn(L)Br_2]$ (A_7)	Zinc bromide	Yellow (Crystal)	65.49	41.26(41.45)	3.85(3.87)	5.36(5.37)

* L = *N*,*N*'-bis(4-Methoxybenzaldehyde)ethylenediamine, L_1 = *N*-(4-Methoxybenzylidene)ethylenediamine.

Table 3. IR spectral bands (cm^{-1}) of the Schiff base and its metal complexes.

Compound	ν(NH_2)	ν(OH)	ν(COO^-)	ν(C=N)	ν(ClO_4^-)	ν(M-N)
L	-	-	-	1639	-	-
$[Cu(L)(ClO_4)(CH_3OH)]\cdot ClO_4$ (A_1)	-	3199	-	1678	1075, 1016, 619	515
$[Cu(L)(CH_3COO)_2]\cdot 3H_2O$ (A_2)	-	3298	1553, 1416	1683	-	514
$[Cu(L_1)Cl_2]\cdot H_2O$ (A_3)	3261	-	-	1637	-	524
$[Zn(L_1)Cl_2]$ (A_4)	3281	-	-	1628	-	473
$[Zn(L)Cl_2]$ (A_5)	-	-	-	1635	-	464
$[Zn(L)I_2]$ (A_6)	-	-	-	1631	-	421
$[Zn(L)Br_2]$ (A_7)	-	-	-	1634	-	422

The experiments were carried out in independent triplicate (n = 3). The volume of DMSO corresponding to the highest dose of the compounds tested (final concentration of 1, 2, 3.2, 3.8% DMSO) was used as a negative control and was found to be inactive, showing that the latter is not involved in the results obtained from the compounds. The plates were incubated for 24 hours at a temperature of 37 °C before reading for the antibacterial test and at 35 °C for the antifungal tests. At the end of the incubation, the optical density (OD) 600 nm was measured using a microplate reader (Synergy Mx, Biotek) [24]. The antibacterial activity was evaluated by determination of the minimum inhibitory concentration (MIC) values of the compounds. The MIC is defined as the lowest concentration inhibiting the visible growth of the organism.

2.4. Kinetic of the hydrolysis of phosphodiesters of complexes

The solutions used, the substrate bis(4-nitrophenyle) phosphate (50 mm, BNPP), potassium chloride (KCl, 0.25 M) and a borate buffer solution (0.1 M) at pH = 8.5 are prepared in distilled water. Due to the low solubility in water, the complexes studied are prepared in a mixture of water and methanol in the proportions (1/10, v/v, 100 mM). The study of the catalytic activity of phosphodiesters was carried out using sterile 96 well polypropylene microplates filled with a micropipette according to the protocol described by Selmeczi *et al.* [25]. In a typical experiment, freshly prepared solutions of complexes (50 µL), a KCl (50 µL) solution are injected to maintain the ionic strength and the medium buffered by 50 µL of a borate buffer solution. 50 µL of the substrate is added to this mixture; the transparent solution turns yellow after adding the substrate. The final volume of each well is 200 µL. BNPP hydrolysis of the studied complexes gives *p*-nitrophenol (PNP) and *p*-nitrophenyl phosphate (PNPP). The progress of the reaction was monitored by the absorbance change visible at 400 nm due to the release of the 4-nitrophenolate anion for 2 h at a temperature of 27 °C.

3. Results and discussion

3.1. Characterization of the Cu(II) and Zn(II) complexes

The IR spectra show the appearance of characteristic bands of the ligand and those of the the molecules of water, acetate, and perchlorate groups (Table 3). Among the bands of the L ligand, we are particularly interested in those related to the ν(C=N) vibrations of the azomethine group. This absorption band has undergone a shift compared to that of the ligand, which is located at 1639 cm^{-1}. This shift occurs at high frequencies for the perchlorate and copper acetate complexes, respectively, at 1669 and 1683 cm^{-1} [26-29], and towards low frequencies for the zinc and copper chloride complexes, respectively, at 1635, 1631, 1634, and 1629 cm^{-1} [30-33]. The shift of this band and the presence of weak bands towards low frequencies confirm the coordination of the nitrogen atom N of the imine group with the different metals. In the infrared spectrum of the A_1 complex, in addition to the L ligand bands, absorption bands are observed at 1075, 1013 and 619 cm^{-1} attributed to vibrations of the bound perchlorate ion. We also note the ν(OH) absorption band of methanol at 3197 cm^{-1}. On the A_2 complex spectrum, the $\nu_{as}(COO)$ and $\nu_s(COO)$ bands are located at 1597 and 1416 cm^{-1}, respectively [34,35]. The difference between $\nu_{as}(COO)$ and $\nu_s(COO)$ equal to 181 cm^{-1} proves that acetate is monodentate [36]. Band at 3296 cm^{-1} is attributed to ν(OH) water molecules [37,38]. In the spectra of the A_3 and A_4 complexes, the two fine bands at 3261 and 3281 cm^{-1} are attributed to ν(NH_2) of the amine group, respectively [39,40]. The appearance of this band with that of the azomethine group and the absence of the ν band (C=O) show a partial hydrolysis of the L ligand.

The conductivity measurements (A_1, A_2 and A_3) of the complexes were carried out in a millimolar solution (1×10^{-3} M) of DMSO. Two measurements are taken within a fortnight interval to monitor the stability of the complexes in DMSO. The molar conductance values of the copper complexes were measured both when freshly prepared and after 15 days. For $[Cu(L)(ClO_4)(CH_3OH)]\cdot ClO_4$ (A_1), the molar conductance was initially 54 µS/cm and slightly decreased to 51 µS/cm after 15 days. In the case of $[Cu(L)(CH_3COO)_2]\cdot 3H_2O$ (A_2), the value remained constant at 17 µS/cm over the same period. Interestingly, $[Cu(L_1)Cl_2]\cdot H_2O$ (A_3) exhibited a slight increase in molar conductance, from 24 to 27 µS/cm after 15 days. These conductimetric results of fresh solutions indicate that the A_2 and A_3 complexes are neutral electrolytes, which indicates the coordination of acetates and chloride atoms with copper [41]. For complex A_1, the value of the conductivity obtained is 54 µS/cm. These data are in agreement with an electrolyte type 1:1 and indicate that one of the perchlorate ions is free and plays a role of counter-ion [42]. These results complete the infrared data of the complexes. After 15 days, a slight shift in the conductimetric data of these complexes is observed, which shows the stability of the complexes in DMSO.

The analysis of the ^1H NMR spectra shows the presence of five signals present in the ligand. Singlets at δ 3.7 and 3.8 ppm that incorporate 6 and 4 protons, respectively, are assigned to protons of the methoxyl (CH_3-) and ethyl (CH_2-CH_2) groups. The doublets at δ 7.66-6.98 ppm or δ 7.65 and 6.98 ppm are attributed to the protons of the aromatic nucleus.

Table 4. UV-vis spectra of the Schiff base ligand and its Cu(II) and Zn(II) complex.

Compound	Absorption (nm)	Band assignments
L	215, 270	π-π*, n-π*
$[Cu(L)(ClO_4)(CH_3OH)]\cdot ClO_4$	223, 275	π-π*, n-π*
	402	LMCT
	620	*d–d*
$[Cu(L)(CH_3COO)_2]\cdot 3H_2O$	220, 270	π-π*, n-π*
	660	d–d
$[Cu(L_1)Cl_2]\cdot H_2O$	220, 285	π-π*, n-π*
	360	LMCT
	690	*d–d*
$[Zn(L)Cl_2]$	216, 2764	π-π*, n-π*
$[Zn(L)I_2]$	221, 279	π-π*, n-π*
$[Zn(L)Br_2]$	220, 275	π-π*, n-π*

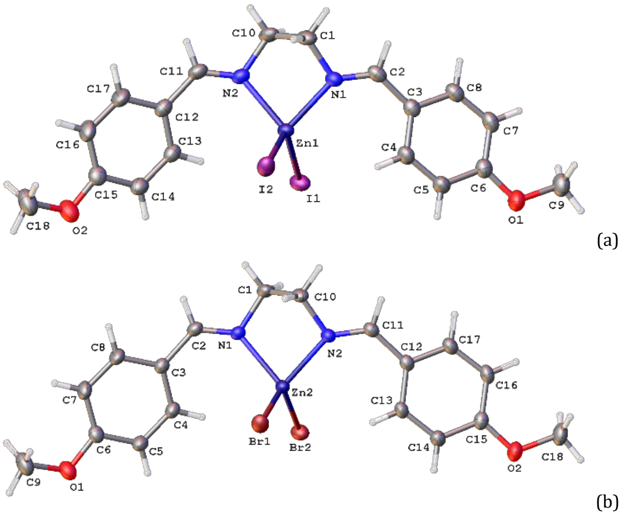

Figure 1. Molecular structure of the zinc (a) iodide and (b) bromide complexes.

The singlet attributed to imine protons at δ 8.19 ppm for the ligand and at δ 8.25 ppm (δ 8.24 ppm) for the complexes confirms the participation of imine nitrogen in the zinc coordination [43,44].

The electronic spectra of the complexes are recorded in freshly prepared ethanol solution at different concentrations, 1×10^{-5} M for low absorbances (200-400 nm) and 1×10^{-3} M for high absorbances (500-800 nm) (Table 4). These spectra show absorption bands between 200 and 300 nm attributed to the $\pi \rightarrow \pi^*$ absorptions of the aromatic nucleus and $n \rightarrow \pi^*$ transitions of the imine group contained in the ligand [45]. These transition bands undergo a bathochromic effect compared to those of the ligand because of the presence of different acid, basic or halide auxochromes (OH, NH_2, Cl, I, and Br) in the complexes. The bands at 402 and 360 nm on the spectra of the A_1 and A_3 complexes are attributed to ligand-metal charge transfer (LMCT) [46]. In addition to these bands, the d–d transitions of the copper complexes are also observed at 620 nm (A_1), 660 nm (A_2) and 690 nm (A_3). These bands correspond to the transition bands of an octahedral or square-plane copper complex [47]. For complexes A_5 A_6 and A_7 the *d* - *d* transitions of zinc cannot be observed because the *d* subshell is full (d^{10}).

3.2. Crystallographic study of zinc complexes

The crystallographic study of the zinc iodide and bromide complexes shows that they crystallize in the monoclinic system of space group $P2_1/c$. The lattice parameters are as follows: a = 10.4567(10) Å; b = 13.28610(10) Å; c = 15.4349(10) Å; β = 96.4300(10) for the A_6 complex and a = 10.3007(17) Å; b = 13.0071(18) Å; c = 15.0084(2) Å; β = 97.3057(2) ° for the A_7 complex. The unit cell of each complex consists of four molecules (Z = 4). The crystal structure of the complexes shows that zinc is tetracoordinated with the two nitrogen atoms of the azomethine group contained in the ligand, stabilized by two halide atoms (Figure 1). The crystal structure of the zinc chloride complexes A_4 and A_5 has been reported in a previous article [48]. The values of the bond angles around zinc(II) I2–Zn–I1, I2–Zn–N2, I1–Zn–N1, N2–Zn–N1, N1–Zn–N2, N1–Zn–Br2, N2–Zn–Br1 and Br2–Zn–Br1 are, respectively, 118.62(2)°, 108.64(10)°, 116.17(10)°, 84.71(15)°, 84.54(7)°, 114.94(6)°, 108.89(6)° and 117.58(14)° (Table 5). To explain the geometry around the Zn(II) ion, we used the distortion index or the tetragonality parameter (τ^4) [49] calculated from the formula: $\tau^4 = [360° - (\alpha + \beta)]/141°$, where α and β are the two largest angles formed by the donor atoms and the metal center (Figure 1). A value of $\tau^4 = 1$ gives a regular tetrahedral geometry, while for a value of $\tau^4 = 0$ we have a perfect square plane [50]. In our study, the value of τ^4 is 0.8878 for the A_6 complex and 0.9041 for the A_7 complex, which indicates a slightly distorted tetrahedral geometry. On the other hand, the sum of the angles around the zinc(II) is equal to 428.14° (A_6) and 425.95° (A_7), we also note the variation of the angles around the Zn(II) ion with respect to the valence angle of 109.5°. These data agree with the value of τ^4 found and confirm the slightly distorted tetrahedral geometry of the zinc complexes. This variation in the bond angles around the zinc compared to those around a regular tetrahedron is due to the steric effects of the halide atoms (I, Br). The bond lengths Zn–N1, Zn–N2, Zn–I1 and Zn–I2 in the complex A_6 are, respectively, equal to 2.078(3), 2.088(4), 2.5461(16) and 2.5387(16) Å (Table 6) and are in good agreement with the lengths of the corresponding bonds in other zinc(II) complexes with a tetrahedral ZnN_2I_2 chromophore [51]. For the bromide complex, the Zn–N1 (2.0836(18) Å) and Zn–N2 (2.0693(18) Å) bond lengths are similar to those previously reported by Khalaji [52].

Table 5. Selected bond angles for the zinc complexes.

A$_6$				A$_7$			
Atom	**Atom**	**Atom**	**Angle (°)**	**Atom**	**Atom**	**Atom**	**Angle (°)**
I2	Zn1	I1	118.62(2)	Br1	Zn2	Br2	117.576(14)
N1	Zn1	I1	116.17(10)	N1	Zn2	Br1	109.16(5)
N1	Zn1	I2	108.67(10)	N1	Zn2	Br2	114.94(6)
N1	Zn1	N2	84.71(15)	N2	Zn2	Br1	108.89(6)
N2	Zn1	I1	114.96(10)	N2	Zn2	Br2	116.99(5)
N2	Zn1	I2	108.64(10)	N2	Zn2	N1	84.54(7)
C6	O1	C9	117.2(5)	C6	O1	C9	117.3(2)
C15	O2	C18	117.7(5)	C15	O2	C18	117.6(2)
C1	N1	Zn1	104.7(3)	C1	N1	Zn2	106.77(14)
C2	N1	Zn1	138.5(3)	C2	N1	Zn2	134.66(16)
C2	N1	C1	116.6(4)	C2	N1	C1	117.54(19)
C10	N2	Zn1	106.1(3)	C10	N2	Zn2	105.08(14)
C11	N2	Zn1	134.5(3)	C11	N2	Zn2	138.16(16)
C11	N2	C10	118.1(4)	C11	N2	C10	116.41(19)
N1	C1	C10	108.9(4)	N1	C1	C10	108.9(2)
N1	C2	C3	128.5(4)	N1	C2	C3	126.9(2)

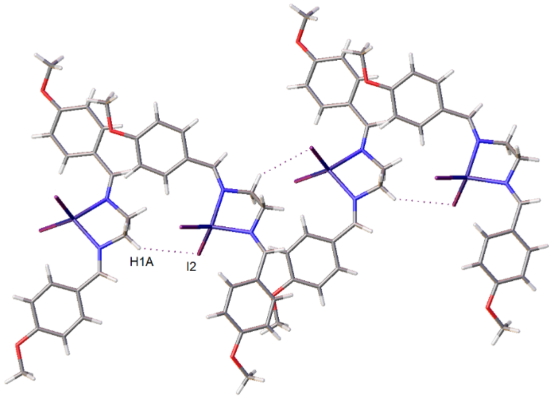

Figure 2. Infinite chain structure of the zinc iodide complex stabilized by hydrogen bonds of the C–H···I type ($d_{\text{I2-H1A}}$ = 3.096 Å).

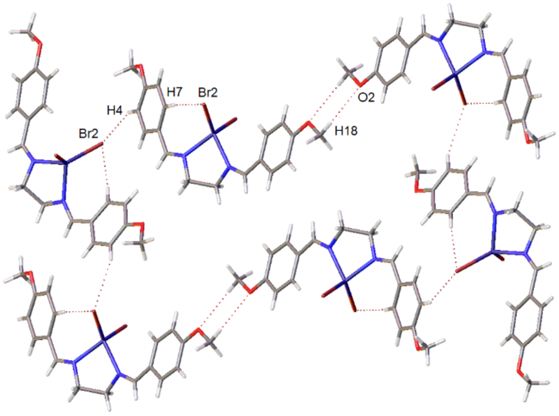

Figure 3. Structure of complex zinc bromide showing C–H···Br and C–H···O intermolecular hydrogen bonds (dashed) ($d_{\text{Br2-H4}}$ = 3.005 Å, $d_{\text{Br2-H7}}$ = 3.029 Å, $d_{\text{O2-H18}}$ = 2.633 Å).

The dihedral angles of the complex A$_6$ C1–N1–C2–C3 and C10–N2–C11–C12 are respectively equal to 179.1(2)° and 179.9(2)° indicate an almost planar configuration of this fraction of the complex. The monomers of the zinc complexes are linked by intermolecular hydrogen bonds of type C1–H1A···I2, C10–H···Br1 and C18–H···O2 (Figure 2 and 3). These intermolecular hydrogen bonds strengthen the cohesion and stability of the complex, thus giving it a supramolecular structure.

3.3. Study of the fluorescence of ligand and zinc complexes

The fluorescence spectra of ligand L and these zinc complexes at 8×10^{-4} M are represented in Figure 4. These spectra show the presence of two emission bands: the fine band towards 392 nm attributed to the fluorescence band due to the group OH in methanol and the broad band towards 400 nm due to the emission of the different compounds tested. These emission spectra reveal that the intensity of the fluorescence varies according to the concentration, this variation increases with increasing concentration [53]. The analysis of the fluorescence spectra of the ligand and of the zinc complexes shows a decrease in the intensity of the fluorescence of the complexes of chloride, iodide and bromide of zinc compared to that of the ligand passing from 225610 to 187540; 161510; 436160, respectively. It appears from the emission spectra that the intensity of the fluorescence decreased considerably during the formation of zinc complexes. The decrease in intensity is due to magnetic disturbance and electronic energy transfers, but also to the presence of halide atoms in complexes [54].

Table 6. Selected bond lengths for the zinc complexes.

A_6			A_7		
Atom	**Atom**	**Length (Å)**	**Atom**	**Atom**	**Length (Å)**
I1	Zn1	2.5461(6)	Br1	Zn2	2.3449(4)
I2	Zn1	2.5387(6)	Br2	Zn2	2.3535(4)
Zn1	N1	2.078(3)	Zn2	N1	2.0836(18)
Zn1	N2	2.088(4)	Zn2	N2	2.0693(18)
O1	C6	1.353(6)	O1	C6	1.354(3)
O1	C9	1.449(7)	O1	C9	1.434(3)
O2	C15	1.348(7)	O2	C15	1.353(3)
O2	C18	1.440(8)	O2	C18	1.441(3)
N1	C1	1.468(6)	N1	C1	1.474(3)
N1	C2	1.272(6)	N1	C2	1.267(3)
N2	C10	1.471(6)	N2	C10	1.472(3)
N2	C11	1.262(6)	N2	C11	1.276(3)

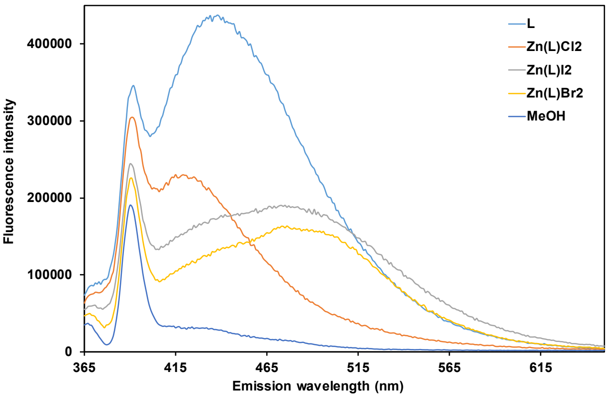

Figure 4. Fluorescence emission spectra of the ligand and of the zinc complexes.

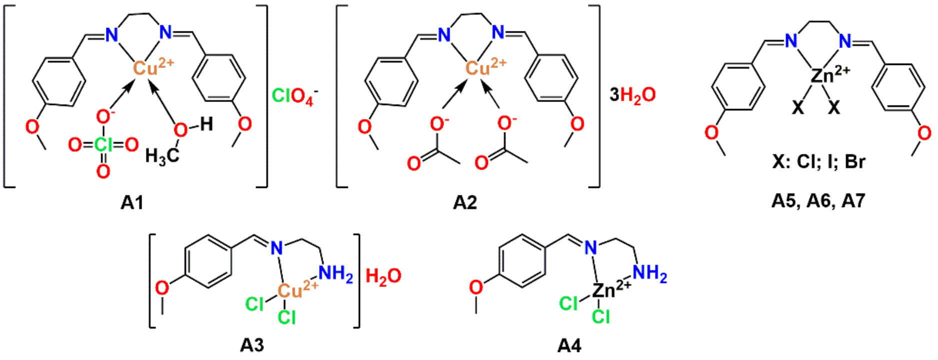

Scheme 2. Proposed structure for zinc complexes (A_1-A_7).

3.4. Proposed structures for complexes

Based on infrared, UV-visible spectroscopic data and elemental analysis of the complexes, we have proposed the structures of copper complexes A_1, A_2, A_3 shown in Scheme 2, the geometry around the copper is square plan. This geometry is supported by the presence of the *d-d* band around 600 nm characteristic of a square planar copper complex. For the zinc complexes, we note a tetrahedral geometry in which the zinc is coordinated via the two nitrogen atoms of the imine group.

3.5. Antimicrobial activity

3.5.1. Antibacterial activity

The results of the preliminary tests of ligand L and its metal compounds are listed in Table 7. The results of this study reveal that the compounds tested have weak antibacterial activity on the two bacteria used with MIC, which are greater than 1000 µM. These values obtained are very high compared to those obtained by Kumar [55], but they are comparable to those found by Matar [56] on Schiff base ligands synthesized from condensation of benzaldehyde derivatives and 3,3'-diaminodipropylamine on different bacterial strains. The high inhibitory concentrations found compared to certain antibiotics such as standard ciprofloxacin allow us to conclude that the compounds tested have very weak antibacterial activity on Gram (-) *Pseudomonas aeruginosa* and Gram (+) *Streptococcus pyogenes* bacteria [57].

3.5.2. Antifungal activity

The MICs of the compounds tested against *Candida albicans* (DSM 10697) fungus are listed in Table 7. Analysis of these results shows that the copper complexes have significant activity with MIC equal to 245.1 µM. Their antifungal activity is much higher than that of zinc complexes and the free ligand (MIC > 900 µM). This decrease may be due to the presence of water molecules in the structure of these complexes [58].

Table 7. Antimicrobial activity of ligand L and its metal complexes.

Compound	**Concentration (mM)**	***P. aeruginosa***	***S. pyogenes***	***C. albicans***
L	100	>1000	>1000	>990.1
$[Cu(L)(ClO_4)(CH_3OH)]\cdot ClO_4$	50	>1000	>1000	245.1
$[Cu(L)(CH_3COO)_2]\cdot 3H_2O$	50	>1000	>1000	245.1
$[Cu(L_1)Cl_2]\cdot H_2O$	50	>1000	>1000	245.1
$[Zn(L)Cl_2]$	100	>1000	>1000	990.1
$[Zn(L)I_2]$	100	>1000	>1000	990.1
$[Zn(L)Br_2]$	100	>1000	>1000	990.1
Ciprofloxacin	100	0.18	6.25	-
Fluconazole	100	-	-	7.8

Table 8. Kinetic data of BNPP hydrolysis of zinc complexes of ligand L.

Complex	**V (mol/L s)**	**k_{obs} (1/s)**
$[Zn(L)Cl_2]$	1.00×10^{-5}	8.00×10^{-4}
$[Zn(L)I_2]$	1.18×10^{-5}	9.44×10^{-4}
$[Zn(L)Br_2]$	8.94×10^{-6}	7.15×10^{-4}

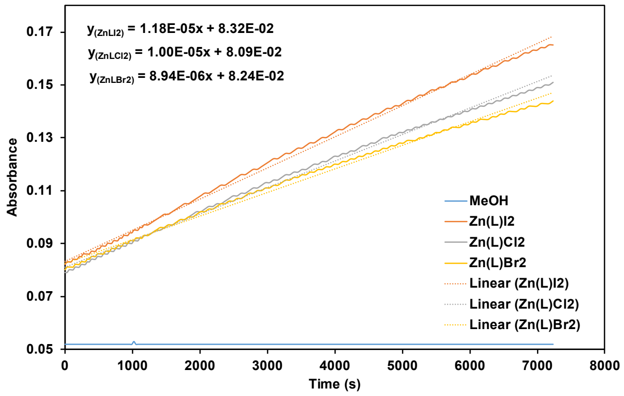

Figure 5. Comparative absorption profile due to *para*-nitrophenol formation (λ_{max} = 400 nm) after the addition of BNPP to the complexes.

The values obtained are very high, compared to those of *Sani et al.* [59] in the study of the antifungal activity of the tetradentate ligand derived from ethylenediamine and 4-(benzeneazo)salicylaldehyde and its Cu(II) complexes; Ni(II) and Zn(II) on the fungi *A. flavus* and *C. albicans*. The antifungal tests found, compared to those of a standard antibiotic, fluconazole, are very high, which shows their low activity on the fungus *C. albicans* [59].

3.6. Study of the hydrolysis of phosphodiesters by complexes A5, A6, and A7

Reactions were determined from the slope of the absorbance versus time curve (Figure 5). The values of the observed initial rates (V) and first-order rate constants (k_{obs} = V/[BNPP]) for the appearance of the *para*-nitrophenolate anion are listed in Table 8. The comparative study of these values of k_{obs} and formation speeds shows that the zinc iodide complex of the ligand has a constant of 9.44×10^{-4} 1/s higher than that of the zinc chloride and zinc bromide complexes (8×10^{-4} mol/L s; 7.15×10^{-4} 1/s). These formation rate values show that the compounds tested have a catalytic activity for the BNPP hydrolysis reaction. This allows us to say that the complexes studied can considerably accelerate the breaking of the phosphoester bond of BNPP.

4. Conclusions

In summary, we have prepared a series of seven new metal complexes with a Schiff base obtained by condensation of *p*-anisaldehyde and ethylenediamine using alcohol as the solvent. The synthesized complexes have a distorted tetrahedral environment around zinc and a square plane for copper complexes. We also studied the fluorescence of ligand L and its zinc complexes. This decrease in fluorescence intensity is due to the presence of halide ions in the complex structures or to photo-induced energy transfer. It has also been shown that the synthesis of complexes of this ligand by reflux heating or vigorous agitation leads to hydrolysis of the ligand. The results of the microbial activity reveal that the ligands and complexes studied have very low antimicrobial activity in bacterial strains (Gram-negative *Pseudomonas aeruginosa* and Gram-positive *Streptococcus pyogenes*) and the fungus *Candida albicans*. Analysis of the data obtained from absorbance *vs*. time curves shows that the zinc complexes tested can accelerate the breakdown of the P-O bond of *bis*-*para*-nitrophenylphosphate.

Acknowledgements

The authors gratefully acknowledge Aix Marseille University, The Laboratoire Bioscience Service 332, especially Dr. Michel Giorgi, Dr. Gregory Excoffier, Dr. Marc Maresca, Dr. Bruno Faure and Dr. Jalila Simaan for the XRD analyses, elemental microanalyses, antimicrobial studies, and follow-up of the work.

Supporting information S

CCDC-2112981 ($C_{18}H_{20}I_2N_2O_2Zn$) and CCDC-2063276 ($C_{18}H_{20}Br_2N_2O_2Zn$) contain the supplementary crystallographic data for this paper. These data can be obtained free of charge via www.ccdc.cam.ac.uk/data_request/cif , or by e-mailing data_request@ ccdc.cam.ac.uk, or by contacting The Cambridge Crystallographic Data Centre, 12 Union Road, Cambridge CB2 1EZ, UK; fax: +44(0)1223-336033.

Disclosure statement DS

Conflict of interest: The authors declare that they have no conflict of interest.
Ethical approval: All ethical guidelines have been adhered.
Sample availability: Samples of the compounds are available from the author.

CRediT authorship contribution statement

Conceptualization: Tidiane Diop, Aminata Diasse-Sarr; Methodology: Adrienne Ndiolene, Tidiane Diop; Software : Mouhamadou Sembene Boye, Michel Giorgi; Validation : Adrienne Ndiolene, Tidiane Diop; Formal Analysis: Adrienne Ndiolene; Investigation : Adrienne Ndiolene, Tidiane Diop; Resources: Tidiane Diop, Aminata Diasse-Sarr ; Data Curation: Adrienne Ndiolene, Michel Giorgi; Writing – Original Draft : Adrienne Ndiolene, Tidiane Diop; Writing - Review and Editing: Mouhamadou Sembene Boye, Aminata Diasse-Sarr; Visualization: Adrienne Ndiolene; Supervision : Tidiane Diop, Aminata Diasse-Sarr, Bruno Faure; Project Administration: Aminata Diasse-Sarr.

Funding

This scientific work was supported by the cooperation of Senegal Marseille with the Erasmus International Credit Mobility bourse for nine months.

ORCID and Email

Adrienne Ndiolene
adrienne.ndiolene@ucad.edu.sn
https://orcid.org/0009-0004-2411-8836
Tidiane Diop
tidiane3.diop@ucad.edu.sn
https://orcid.org/0000-0003-1098-451X
Mouhamadou Sembene Boye
mouhasboye@hotmail.com
https://orcid.org/0009-0000-8447-6409
Bruno Faure
bruno.faure@univ-amu.fr
https://orcid.org/0000-0003-2117-8310
Aminata Diasse-Sarr
aminatadiasse.sarr@ucad.edu.sn
https://orcid.org/0000-0002-4143-4281
Michel Giorgi
michel.giorgi@univamu.fr
https://orcid.org/0000-0002-4367-1985

References

[1]. Golcu, A.; Tumer, M.; Demirelli, H.; Wheatley, R. A. Cd(II) and Cu(II) complexes of polydentate Schiff base ligands: synthesis, characterization, properties and biological activity. *Inorg. Chim. Acta* **2005**, *358* (6), 1785–1797.

[2]. Justin Dhanaraj, C.; Sivasankaran Nair, M. Synthesis, characterization, and antimicrobial studies of some Schiff-base metal(II) complexes. *J. Coord. Chem.* **2009**, *62* (24), 4018–4028.

[3]. Badwaik, V.; Deshmukh, R.; Aswar, A. Transition metal complexes of a Schiff base: synthesis, characterization, and antibacterial studies. *J. Coord. Chem.* **2009**, *62* (12), 2037–2047.

[4]. Keypour, H.; Shayesteh, M.; Rezaeivala, M.; Chalabian, F.; Elerman, Y.; Buyukgungor, O. Synthesis, spectral characterization, structural investigation and antimicrobial studies of mononuclear Cu(II), Ni(II), Co(II), Zn(II) and Cd(II) complexes of a new potentially hexadentate N2O4 Schiff base ligand derived from salicylaldehyde. *J. Mol. Struct.* **2013**, *1032*, 62–68.

[5]. Bhaskar, R.; Salunkhe, N.; Yaul, A.; Aswar, A. Bivalent transition metal complexes of ONO donor hydrazone ligand: Synthesis, structural characterization and antimicrobial activity. *Spectrochim. Acta A: Mol. Biomol. Spectrosc.* **2015**, *151*, 621–627.

[6]. Neelakantan, M.; Esakkiammal, M.; Mariappan, S.; Dharmaraja, J.; Jeyakumar, T. Synthesis, Characterization and Biocidal Activities of Some Schiff Base Metal Complexes. *Indian J. Pharm. Sci.* **2010**, *72* (2), 216.

[7]. Rajavel, R.; Vadivu, M. S.; Anitha, C. Synthesis, Physical Characterization and Biological Activity of Some Schiff Base Complexes. *J. Chem.* **2008**, *5* (3), 620–626.

[8]. Mishra, A. P.; Khare, M.; Gautam, S. K. Synthesis, physico-chemical characterization, and antibacterial studies of some bioactive Schiff bases and their metal chelates. *Synth. React. Inorg. Met.-Org. Chem.* **2002**, *32* (8), 1485–1500.

[9]. Zafar, H.; Ahmad, A.; Khan, A. U.; Khan, T. A. Synthesis, characterization and antimicrobial studies of Schiff base complexes. *J. Mol. Struct.* **2015**, *1097*, 129–135.

[10]. Saranya, J.; Jone Kirubavathy, S.; Chitra, S.; Zarrouk, A.; Kalpana, K.; Lavanya, K.; Ravikiran, B. Tetradentate Schiff Base Complexes of Transition Metals for Antimicrobial Activity. *Arab. J. Sci. Eng.* **2020**, *45* (6), 4683–4695.

[11]. Chew, K.; Tarafder, M.; Crouse, K. A.; Ali, A.; Yamin, B.; Fun, H. Synthesis, characterization and bio-activity of metal complexes of bidentate N–S isomeric Schiff bases derived from S-methyldithiocarbazate (SMDTC) and the X-ray structure of the bis[S-methyl-β-N-(2-furyl-methylketone)dithiocarbazato]cadmium(II) complex. *Polyhedron* **2004**, *23* (8), 1385–1392.

[12]. Pahonțu, E.; Proks, M.; Shova, S.; Lupașcu, G.; Ilieș, D.; Bărbuceanu, S.; Socea, L.; Badea, M.; Păunescu, V.; Istrati, D.; Gulea, A.; Drăgănescu, D.; Pîrvu, C. E. Synthesis, characterization, molecular docking studies and *in vitro* screening of new metal complexes with Schiff base as antimicrobial and antiproliferative agents. *Applied Organomet. Chem.* **2019**, *33* (11), e5185 https://doi.org/10.1002/aoc.5185.

[13]. Mishra, N.; Poonia, K.; Soni, S. K.; Kumar, D. Synthesis, characterization and antimicrobial activity of Schiff base Ce(III) complexes. *Polyhedron* **2016**, *120*, 60–68.

[14]. Pramanik, H. A.; Paul, P. C.; Mondal, P.; Bhattacharjee, C. R. Mixed ligand complexes of cobalt(III) and iron(III) containing N2O2-chelating Schiff base: Synthesis, characterisation, antimicrobial activity, antioxidant and DFT study. *J. Mol. Struct.* **2015**, *1100*, 496–505.

[15]. Islam, S.; Roy, A. S.; Mondal, P.; Mubarak, M.; Mondal, S.; Hossain, D.; Banerjee, S.; Santra, S. Synthesis, catalytic oxidation and antimicrobial activity of copper(II) Schiff base complex. *J. Mol. Catal. A: Chem.* **2011**, *336* (1-2), 106–114.

[16]. Shebl, M.; Khalil, S. M.; Ahmed, S. A.; Medien, H. A. Synthesis, spectroscopic characterization and antimicrobial activity of mono-, bi- and tri-nuclear metal complexes of a new Schiff base ligand. *J. Mol. Struct.* **2010**, *980* (1-3), 39–50.

[17]. Prakash, A.; Singh, B. K.; Bhojak, N.; Adhikari, D. Synthesis and characterization of bioactive zinc(II) and cadmium(II) complexes with new Schiff bases derived from 4-nitrobenzaldehyde and acetophenone with ethylenediamine. *Spectrochim. Acta A: Mol. Biomol. Spectrosc.* **2010**, *76* (3-4), 356–362.

[18]. Marchetti, F.; Pettinari, C.; Pettinari, R.; Cingolani, A.; Leonesi, D.; Lorenzotti, A. Group 12 metal complexes of tetradentate N2O2–Schiff-base ligands incorporating pyrazole. *Polyhedron* **1999**, *18* (23), 3041–3050.

[19]. Sheldrick, G. M. *SHELXT*– Integrated space-group and crystal-structure determination. *Acta Crystallogr. A. Found Adv.* **2015**, *71* (1), 3–8.

[20]. Dolomanov, O. V.; Bourhis, L. J.; Gildea, R. J.; Howard, J. A.; Puschmann, H. *OLEX2*: a complete structure solution, refinement and analysis program. *J. Appl. Crystallogr.* **2009**, *42* (2), 339–341.

[21]. Ndiolene, A.; Diop, T.; Sembene Boye, M.; Maris, T.; Diasse-Sarr, A. Synthesis, Spectroscopic Studies and Crystal Structures of N, N'-bis (4-methoxybenzylidene) Ethylenediamine and an Its New Cadmium (II) Complex. *AJHC.* **2020**, *6* (2), 30.

[22]. Yu, T.; Su, W.; Li, W.; Hong, Z.; Hua, R.; Li, M.; Chu, B.; Li, B.; Zhang, Z.; Hu, Z. Z. Synthesis, crystal structure and electroluminescent properties of a Schiff base zinc complex. *Inorganica Chim. Acta* **2006**, *359*, 2246–2251.

[23]. Olleik, H.; Yacoub, T.; Hoffer, L.; Gnansounou, S. M.; Benhaiem-Henry, K.; Nicoletti, C.; Mekhalfi, M.; Pique, V.; Perrier, J.; Hijazi, A.; Baydoun, E.; Raymond, J.; Piccerelle, P.; Maresca, M.; Robin, M. Synthesis and Evaluation of the Antibacterial Activities of 13-Substituted Berberine Derivatives. *Antibiotics* **2020**, *9* (7), 381.

[24]. Olleik, H.; Yahiaoui, S.; Roulier, B.; Courvoisier-Dezord, E.; Perrier, J.; Pérès, B.; Hijazi, A.; Baydoun, E.; Raymond, J.; Boumendjel, A.; Maresca, M.; Haudecoeur, R. Aurone derivatives as promising antibacterial agents against resistant Gram-positive pathogens. *Eur. J. Med. Chem.* **2019**, *165*, 133–141.

[25]. Selmeczi, K.; Giorgi, M.; Speier, G.; Farkas, E.; Réglier, M. Mono- versus Binuclear Copper(II) Complexes in Phosphodiester Hydrolysis. *Eur. J. Inorg. Chem.* **2006**, *2006* (5), 1022–1031.

[26]. Arslan, T.; Öğretir, C.; Tsiouri, M.; Plakatouras, J. C.; Hadjiliadis, N. Interactions of trivalent lanthanide cations with a hexadentate Schiff base derived from the condensation of ethylenediamine with 8-hydroxyquinoline-2-carboxaldehyde. *J. Coord. Chem.* **2007**, *60* (6), 699–710.

[27]. Yu, Y.; Xian, H.; Liu, J.; Zhao, G. Synthesis, Characterization, Crystal Structure and Antibacterial Activities of Transition Metal(II) Complexes of the Schiff Base 2-[(4-Methylphenylimino)methyl]-6-methoxyphenol. *Molecules* **2009**, *14* (5), 1747–1754.

[28]. Ali, O. A.; El-Medani, S. M.; Ahmed, D. A.; Nassar, D. A. Synthesis, characterization, fluorescence and catalytic activity of some new complexes of unsymmetrical Schiff base of 2-pyridinecarboxaldehyde with 2,6-diaminopyridine. *Spectrochim. Acta A: Mol. Biomol. Spectrosc.* **2015**, *144*, 99–106.

[29]. Taha, Z. A.; Ajlouni, A. M.; Al Momani, W.; Al-Ghzawi, A. A. Syntheses, characterization, biological activities and photophysical properties of lanthanides complexes with a tetradentate Schiff base ligand. *Spectrochim. Acta A: Mol. Biomol. Spectrosc.* **2011**, *81* (1), 570–577.

[30]. Mohamed, G. G.; Sharaby, C. M. Metal complexes of Schiff base derived from sulphametrole and o-vanilin. *Spectrochim. Acta A: Mol. Biomol. Spectrosc.* **2007**, *66* (4-5), 949–958.

[31]. Raman, N.; Dhaveethu Raja, J.; Sakthivel, A. Synthesis, spectral characterization of Schiff base transition metal complexes: DNA cleavage and antimicrobial activity studies. *J. Chem. Sci.* **2007**, *119* (4), 303–310.

[32]. Munde, A.; Jagdale, A.; Jadhav, S.; Chondhekar, T. Synthesis, characterization and thermal study of some transition metal complexes of an asymmetrical tetradentate Schiff base ligand. *J. Serb. Chem. Soc.* **2010**, *75* (3), 349–359.

[33]. El-Shafiy, H. F. Synthesis, spectral, photoluminescence, DFT studies and bioassay of new Fe(III), Co(II), Ni(II), Cu(II) and Zn(II) complexes of 1-ethyl-4-hydroxy-3-(nitroacetyl) quinolin-2(1H)-one. *J. Mol. Struct.* **2018**, *1166*, 348–361.

[34]. Nair, M. S.; Joseyphus, R. S. Synthesis and characterization of Co(II), Ni(II), Cu(II) and Zn(II) complexes of tridentate Schiff base derived from vanillin and dl-α-aminobutyric acid. *Spectrochim. Acta A: Mol. Biomol. Spectrosc.* **2008**, *70* (4), 749–753.

[35]. Neelakantan, M.; Rusalraj, F.; Dharmaraja, J.; Johnsonraja, S.; Jeyakumar, T.; Sankaranarayana Pillai, M. Spectral characterization, cyclic voltammetry, morphology, biological activities and DNA cleaving studies of amino acid Schiff base metal(II) complexes. *Spectrochim. Acta A: Mol. Biomol. Spectrosc.* **2008**, *71* (4), 1599–1609.

[36]. Abdel-Rahman, L. H.; El-Khatib, R. M.; Nassr, L. A.; Abu-Dief, A. M. Synthesis, physicochemical studies, embryos toxicity and DNA interaction of some new Iron(II) Schiff base amino acid complexes. *J. Mol. Struct.* **2013**, *1040*, 9–18.

[37]. Abu Al-Nasr, A. K.; Ramadan, R. M. Spectroscopic studies and biological activity of some transition metal complexes of unusual Schiff base. *Spectrochim. Acta A: Mol. Biomol. Spectrosc.* **2013**, *105*, 14–19.

[38]. Zishen, W.; Zhiping, L.; Zhenhuan, Y. Synthesis, characterization and antifungal activity of glycylglycine Schiff base complexes of 3d transition metal ions. *Transition Met. Chem.* **1993**, *18* (3), 291–294 https://doi.org/10.1007/BF00207949

[39]. Abou-Hussen, A. A.; Linert, W. Chromotropism Behavior and Biological Activity of some Schiff Base-Mixed Ligand Transition Metal Complexes. *Synth. React. Inorg. Met.-Org. Nano-Met. Chem.* **2009**, *39* (9), 570–599.

[40]. Sakthilatha, D.; Rajavel, R. Synthesis, characterization and biological studies of homobimetallic Schiff base cu(II) and Ni(II) complexes. *Chem. Sci. Trans.* **2013**, *2*(3), 711-726 http://www.e-journals.in/pdf/V2N3/711-726.pdf

[41]. El-Shafiy, H. F. Synthesis, spectral, photoluminescence, DFT studies and bioassay of new Fe(III), Co(II), Ni(II), Cu(II) and Zn(II) complexes of 1-ethyl-4-hydroxy-3-(nitroacetyl) quinolin-2(1H)-one. *J. Mol. Struct.* **2018**, *1166*, 348–361.

[42]. Shakdofa, M. E. M.; Al-Hakimi, A. N.; A. Elsaied, F.; Alasbahi, S. O. M.; Alkwlini, A. M. A. Synthesis, characterization and bioactivity Zn2+, Cu2+, Ni2+, Co2+, Mn2+, Fe3+, Ru3+, VO2+ and UO22+ complexes of 2-hydroxy-5-((4-nitrophenyl)diazenyl)benzylidene)-2-(p-tolyl-amino)acetohydrazide. *Bull. Chem. Soc. Eth.* **2017**, *31* (1), 75–91. https://doi.org/10.4314/bcse.v31i1.7

[43]. Forouzandeh, F.; Keypour, H.; Zebarjadian, M. H.; Mahmoudabadi, M.; Hosseinzadeh, L.; Karamian, R.; Ahmadi Khoei, M.; Gable, R. W. Synthesis, characterization and X-ray crystal structure of potentially N6O2 coordinating macroacyclic Schiff base ligands and their Mn(II), Zn(II) and Cd(II) complexes; cytotoxic, antibacterial properties and competitive 7Li NMR studies. *Polyhedron* **2019**, *160*, 238–246.

[44]. Hung, W.; Lin, C. Preparation, Characterization, and Catalytic Studies of Magnesium Complexes Supported by NNO-Tridentate Schiff-Base Ligands. *Inorg. Chem.* **2009**, *48* (2), 728–734.

[45]. Sohtun, W. P.; Khamrang, T.; Kannan, A.; Balakrishnan, G.; Saravanan, D.; Akhbarsha, M. A.; Velusamy, M.; Palaniandavar, M. Iron(III) bis-complexes of Schiff bases of *S*-methyldithiocarbazates: Synthesis, structure, spectral and redox properties and cytotoxicity. *Applied Organomet. Chem.* **2020**, *34* (5), e5593 https://doi.org/10.1002/aoc.5593

[46]. Esmaielzadeh, S.; Zarenezhad, E. Copper(II) Schiff Base Complexes with Catalyst Property: Experimental, Theoretical, Thermodynamic and Biological Studies. *ACSi* **2018**, 416–428

[47]. Das, K.; Datta, A.; Sinha, C.; Huang, J.; Garribba, E.; Hsiao, C.; Hsu, C. End-to-End Thiocyanato-Bridged Helical Chain Polymer and Dichlorido-Bridged Copper(II) Complexes with a Hydrazone Ligand: Synthesis, Characterisation by Electron Paramagnetic Resonance and Variable-Temperature Magnetic Studies, and Inhibitory Effects on Human Colorectal Carcinoma Cells. *ChemistryOpen* **2012**, *1* (2), 80–89.

[48]. Ndiolene, A.; Diop, T.; Ndiaye, N.; Boye, M. S.; Michaud, F.; Diasse-Sarr, A. Synthesis, characterization and crystal structure of 4-methoxybenzylidene-based zinc(II) complexes. *Z. fur Naturforsch. B* **2022**, *77* (2-3), 165–169.

[49]. Yang, L.; Powell, D. R.; Houser, R. P. Structural variation in copper(i) complexes with pyridylmethylamide ligands: structural analysis with a new four-coordinate geometry index, τ_4. *Dalton Trans,* **2007**, 955–964. https://doi.org/10.1039/B617136B

[50]. Okuniewski, A.; Rosiak, D.; Chojnacki, J.; Becker, B. Coordination polymers and molecular structures among complexes of mercury(II) halides with selected 1-benzoylthioureas. *Polyhedron* **2015**, *90*, 47–57.

[51]. Chowdhury, T.; Dasgupta, S.; Khatua, S.; Acharya, K.; Das, D. Executing a Series of Zinc(II) Complexes of Homologous Schiff Base Ligands for a Comparative Analysis on Hydrolytic, Antioxidant, and Antibacterial Activities. *ACS. Appl. Bio Mater.* **2020**, *3* (7), 4348–4357.

[52]. Khalaji, A. D.; Weil, M.; Grivani, G.; Akerdi, S. J. Synthesis, characterization, and crystal structure of two zinc(II) halide complexes with the symmetrical bidentate Schiff-base ligand (3,4-MeO-ba)2en. *Monatsh. Chem.* **2010**, *141* (5), 539–543.

[53]. Shebl, M. Synthesis, spectroscopic characterization and antimicrobial activity of binuclear metal complexes of a new asymmetrical Schiff base ligand: DNA binding affinity of copper(II) complexes. *Spectrochim. Acta A: Mol. Biomol. Spectrosc.* **2014**, *117*, 127–137.

[54]. Majumder, A.; Rosair, G. M.; Mallick, A.; Chattopadhyay, N.; Mitra, S. Synthesis, structures and fluorescence of nickel, zinc and cadmium complexes with the N,N,O-tridentate Schiff base N-2-pyridylmethylidene-2-hydroxy-phenylamine. *Polyhedron* **2006**, *25* (8), 1753–1762.

[55]. Kumar, S., Niranjan, M, S.; Chaluvaraju, K, C.; Jamakhandi, C, M and Dayanand Kadadevar. Synthesis and antimicrobial study of some Schiff bases of sulfonamides. *Journal of Current Pharmaceutical Research*, **2010**, 01, 39–42.

[56]. Matar, S. A.; Talib, W. H.; Mustafa, M. S.; Mubarak, M. S.; AlDamen, M. A. Synthesis, characterization, and antimicrobial activity of Schiff bases derived from benzaldehydes and 3,3′-diaminodipropylamine. *Arab. J. Chem.* **2015**, *8* (6), 850–857.

[57]. Yamgar, R. S.; Nivid, Y.; Nalawade, S.; Mandewale, M.; Atram, R. G.; Sawant, S. S. Novel Zinc(II) Complexes of Heterocyclic Ligands as Antimicrobial Agents: Synthesis, Characterisation, and Antimicrobial Studies. *Bioinorg. Chem. Appl.* **2014**, *2014*, 1–10.

[58]. Gull, P.; Ikbal Ahmad Talukdar, M.; Ahmad Dar, O.; Ahmad Malik, M.; Adil Hashmi, A. Synthesis, Spectroscopic Characterization, Coordination, and Antimicrobial Activity of Some Metal Complexes Derived From 1, 2-Diphenylethane-1, 2-dione and Dinitrophenyl Hydrazine Schiff Base Ligand. *Jundishapur J. Nat. Pharm. Prod.* **2018**, *13*(1), e67179. https://doi.org/10.5812/jjnpp.67179

[59]. Sani, M.; Nuraddeen, A. Synthesis, characterization and antibacterial studies of tetradentate schiff base and their metal (II) complexes derived from 4-(Benzeneazo salicylaldehyde and ethylenediamine). *Bayero J. Pure Appl. Sci.* **2019**, *11*, 176.